Journal of Molecular Structure 1247 (2022) 131350

Contents lists available at ScienceDirect

Journal of Molecular Structure

journal homepage: www.elsevier.com/locate/molstr

Synthesis, characterization, DNA binding and anticancer activities of the imidazolidine-functionalized (NHC)Ru(II) complexes

Canbolat Gürses[a,*], Aydın Aktaş[b,c], Sevgi Balcıoğlu[d], Araniy Fadhilah[e], Yetkin Gök[c], Burhan Ateş[e]

[a] İnönü University, Faculty of Science, Department of Molecular Biology and Genetics, 44280, Malatya, Turkey
[b] İnönü University, Health Services Vocational School, 44280, Malatya, Turkey
[c] İnönü University, Faculty of Science, Department of Chemistry, 44280, Malatya, Turkey
[d] Sakarya University of Applied Sciences, Akyazı Vocational School of Health Services, 54400, Sakarya, Turkey
[e] İnönü University, Faculty of Science, Department of Chemistry, Biochemistry and Biomaterials Research Laboratory, 44280, Malatya, Turkey

ARTICLE INFO

Article history:
Received 20 March 2021
Revised 3 August 2021
Accepted 19 August 2021
Available online 24 August 2021

Keywords:
N-heterocyclic carbenes
Ruthenium
Anticancer activity
DNA binding
Fluorescence spectrophotometry
Agarose gel electrophoresis

ABSTRACT

Here, we present a study on the synthesis and biological properties of the ruthenium complexes having naphthyl substituted NHC ligands, which are of great importance for drug development studies. For this purpose, in our study, imidazolidine-functionalized Ru(II)NHC complexes containing naphthyl substitute group were synthesized and *in vitro* anticancer activity as well as DNA binding properties using agarose gel electrophoresis and ethidium bromide fluorescence quenching assay methods were determined in order to understand the biological activities. The Ru(II)NHC complexes were prepared from naphthyl-substituted Ag(I)NHC complexes and $[RuCl_2(p\text{-cymene})]_2$ via the transmetallation method. These new complexes were characterized by using ^{1}H NMR, ^{13}C NMR, FTIR spectroscopic method and elemental analysis techniques. Consequently, complex **1d** showed the highest anticancer activity in terms of IC_{30} and IC_{50} values against HepG2 cell line as 23.9 and 32.84 μM, respectively. Moreover, depending on the data obtained from agarose gel electrophoresis and fluorescence spectrophotometry techniques, **1b** had the highest DNA binding property, which means that **1b** behaved binding DNA in the cell as an intercalative manner rather than disrupting the integrity of cell membrane like **1d**

1. Introduction

The studies on the use of organometallic compounds as anticancer agents are increasing day by day after the first example of cis-diamminedichloroplatinum(II) (known as cisplatin) was approved for clinical use in the late 1970s [1]. Furthermore, platinum-based anticancer drugs are known to have restrictive properties due to dose-limiting toxicities and intrinsic drug resistance [2]. Complexes of other transition metals such as Au [3], Ag [4], Rh [5], Pd [6], Cu [7], and Ru [8] could also be used as anticancer agents like platinum-based complexes. The coordination compounds offer different biological and chemical diversity from organic drugs. This diversity is due to both the chemical behavior of the metal, the types and numbers of ligands coordinated to the metal, and the coordination geometry of the complex [9,10].

Recently studies on ruthenium-based complexes as anticancer agents have been published [11,12]. Ruthenium-based anticancer metallotherapeutics [13,14] are shown as an alternative to other metal complexes in this field due to their different modes of action, they have also been found to have certain benefits over platinum-based therapeutics [15]. Ruthenium-based complexes have desirable properties for medical applications due to their ruthenium scaffolds. These complexes have properties active against certain cisplatin-resistant cell lines and have low side effects due to higher selectivity for cancer cells compared to normal cells. Furthermore, they have higher selective for target cells. They may be associated with selective uptake by tumor compared to healthy tissue. In general, it is thought to be that ruthenium may mimic iron in binding to certain biological molecules [15,16]. However, Alessio described this phenomena from a different perspective. According to the suggestions of Alessio, ruthenium's characteristic related to high affinity for transferrin molecule is confused with the low toxicity effects of ruthenium which mimics iron since ruthenium and iron are in the same group in the periodic table [16–18]. The ruthenium-based organometallic compounds as an anticancer agent have physicochemical and biological properties, intelligently adjustable, and promising candidates for clinical

* Corresponding author.
E-mail address: canbolat.gurses@inonu.edu.tr (C. Gürses).

https://doi.org/10.1016/j.molstruc.2021.131350
0022-2860/

development [19–21]. Recently, clinical trials have been performed for ruthenium-based complexes such as NAMI-A and KP1019 [22].

Functional *N*-heterocyclic carbene (NHC) complexes containing Au, Pt, Ag, Rh, Pd, Cu, and Ru exhibited hopeful pharmacological properties as anticancer agents and most of them showed a high therapeutic effect [23]. Compared to platinum-containing drugs, these non-platinum complexes target different pathways and display different activity methods for the death of cancer cells [24]. Such new metal complexes could have therapeutic potential to effectively treat platinum-based drug-resistant cancer types by reducing the side effects caused by platinum-based drugs. Thus, these metal complexes may have therapeutic potential to reduce the side effects caused by platinum-based drugs and to effectively treat platinum-based drug-resistant cancer styles [1].

The biological activities of organometallic compounds depend on both the metal atom and the properties of the ligands bearing on the metal atom [25,26]. Recently, NHCs are known as flexible ligands in both classical and modern chemistry with their unique features such as strong electron donation ability, steric bulky and electronically adjustable properties and ease of preparation [27–29]. The NHC ligands have attracted the attention of organic and organometallic chemists because of these unique properties. In fact, many studies have recently been reported on the enzyme inhibition effects of NHC precursors that do not contain metal atoms [8,30–33]. These studies revealed that transition metal complexes containing NHC ligands exhibit biological activity.

Metal complexes, including transition metals, have been investigated as an anticancer agent for a long time because of their selectivity to cancer cells, different oxidation states and high stability. These complexes are tried to be developed as an alternative to the first FDA approved drug cisplatin which is a platinum-based drug used in ovarian cancer. However, alternative solutions have been tried to be developed due to its disadvantages such as systemic toxicity, poor dissolution in water and drug resistance development [34]. In the last decades, ruthenium (II) complexes attract attention due to their anticancer properties. The underlying reason for this anticancer feature is that the Ru ion makes Fe mimic and binds to various serum proteins such as albumin and transferrin in organism. Ruthenium complexes show two oxidation states in the organism as Ru^{2+} and Ru^{3+}, and biological properties may vary accordingly [35]. Since DNA is extremely sensitive to oxidation, the most of the studies related to metallonucleases have been focusing on the molecules which cleave DNA oxidatively. Thus, it is so obvious that the structure of the ligand with oxidation level of the metal have a specific characteristic for their interaction with DNA. These ruthenium complexes also show wonderful *in vitro* cytotoxicity [36].

The binding properties and interactions of newly synthesized small molecules to DNA is a significant parameter in the design of novel drugs. DNA-drug interactions basically occur in three ways: a) Through transcription factors and polymerases, b) Through triple helix formed by RNA-DNA interaction, and c) Interaction of small aromatic molecules with DNA double helix. Drug molecules can basically interact with DNA as covalent and non-covalent bonds. In covalent bonds, the molecule interacts with DNA irreversibly, causing cell death. Cisplatin, the most active agent used in the treatment of cancer (high response rates especially in ovarian and small cell lung cancers), is one of the representatives of this group and it shows the effect of chloride groups in its structure with the interaction of nitrogen groups in DNA bases [37].

A cationic intercalator is attracted by DNA, which is electrostatically polyanionic in aqueous solution. The intercalator ion is replaced by a sodium or magnesium cation that is always bound to DNA and establishes a weak electrostatic bond with the outer surface of the DNA. The ligand can slide from this hydrophilic location into the hydrophobic environment between the base pairs. The energy absorbed by the DNA molecule from collisions with the molecules in the solution allows the base pairs to open for a short time. The intercalator can enter this gap during a temporary interval [38]. In order for an intercalator to enter between base pairs, DNA must be partially unwinded to make room between base pairs. The degree of unwinding depends on the intercalator. For instance, ethidium cation, which is the ionic form of ethidium bromide in aqueous solution, is loosening DNA up to 26°, and proflavine opens the auger at an angle of 17° This opening causes the base pairs to separate or relative "rise" of one base pair to the other, so that a 3.4 Å gap occurs in DNA. This loosening causes changes in local structures related to DNA molecule, such as an extension of the DNA double helix or twisting of the base pairs. In recent years, when designing synthesized intercalators, existing intercalators that are often used in chemotherapy are based on, and a number of side chains (ring or straight chain aminoalkyl groups) are attached to them, or hetero/carbocyclic rings are included in the structure while protecting their main structure [39]. In addition, in order to increase the interest of the intercalator to the intercalation area and the time it will spend there, synergetic intercalators to which two or more identical (*e.g.* bisacridines) or different synergetic groups (such as metallo intercalators, cisplatin bound with acridine alkyl chains) that have the feature of intercalator in the structure are also synthesized. The visualization of several physical changes resulting from the interaction of intercalators and biomacromolecules by spectroscopic methods such as UV-GB, NMR, CD and fluorescence enables the structure and functions of these molecules to be determined. Fluorescence spectrophotometer is widely used especially in the analysis of organic compounds that are connected to DNA by intercalation [40].

In this study, we synthesized imidazolidine-functionalized Ru(II)NHC complexes containing a novel series of naphthyl-substituted NHC ligands. The structures of these new Ru(II)NHC complexes were fully characterized by using spectroscopic methods and elemental analysis techniques. The biological activities of these synthesized complexes were investigated in terms of anticancer as well as DNA binding activities using *ct*DNA with ethidium bromide (EtBr) fluorescence quenching and pBR322 plasmid DNA via agarose gel electrophoresis methods.

2. Experimental Part

2.1. Synthesis and Characterization of N*-naphthyl Substituted Ru(II)NHC Complexes*

All imidazolidine-functionalized Ru(II)NHC complexes **1a-d** containing naphthyl substitute group were synthesized by using the standard Schlenk technique. The solvents used were purified by distillation over the drying agents indicated and the solvents used for the synthesis of the complexes were purified by distillation on known drying were transferred under Ar: Et_2O (Na/K alloy), CH_2Cl_2 (P_4O_{10}), hexane, toluene (Na). All other reagents were commercially available from Alfa Aesar and Merck-Sigma-Aldrich Chemical Co. and used without further purification. Melting points were identified in glass capillaries under air with an Electrothermal-9200 melting point apparatus. FT-IR spectra were saved in the range 400–4000 cm^{-1} on Perkin Elmer Spectrum 100 FT-IR spectrometer. Proton (^1H) and Carbon (^{13}C) NMR spectra were recorded using either a Bruker 300 Merkur spectrometer operating at 300 MHz (^1H), 75.47 MHz (^{13}C) in $CDCl_3$ with tetramethylsilane as an internal reference. Elemental analyses were performed by İnönü University Scientific and Technological Research Center (Malatya, TURKEY).

2.1.1. Synthesis of dichloro[1-benzyl-3-naphthyl-imidazolidin-2-ylidene](p-cymene)ruthenium(II), 1a

The complex **1a** was prepared from the chloro[1-benzyl-3-naphthyl-imidazolidin-2-ylidene]silver(I) (0.124 g, 0.28 mmol) and $[RuCl_2(p\text{-cymene})]_2$ in 25 mL dichloromethane. This mixture was stirred for 24 h. at room temperature in dark condition. Then, the mixture was filtered through celite and the solvent were evaporated under vacuum to afford the product as a red solid. The crude product was recrystallized from dichloromethane/diethyl ether (1:3) at room temperature [8, 33]. Yield: 146 mg, (84%). m.p.: 202–203 °C; $\nu_{(CN)}$: 1450 cm^{-1}. Anal. Calc. for $C_{31}H_{34}Cl_2N_2Ru$: C:61.38; H:5.65; N:4.62. Found: C:61.67; H:6.02; N:4.38. ^1H NMR (300 MHz, $CDCl_3$); δ 1.02 and 1.14 (s, 6H, *p*-$CH_3C_6H_4CH(CH_3)_2$); 1.95 (*s*, 3H, *p*-$CH_3C_6H_4CH(CH_3)_2$); 2.64 (*m*, 1H, *p*-$CH_3C_6H_4CH(CH_3)_2$); 3.45, 3.57 and 3.78 (*s*, 4H, NCH_2CH_2N); 5.01 and 5.06 (*s*, 2H, $NCH_2C_6H_5$); 5.19 (*s*, 2H, $NCH_2C_{10}H_7$); 5.27 and 5.40 (*d*, 4H, *J*: 5.9 and 5.9 Hz, *p*-$CH_3C_6H_4CH(CH_3)_2$); 7.20–8.10 (*m*, 12H, Ar–***H***); ^{13}C NMR (300 MHz, $CDCl_3$); δ 18.5 and 19.0 [*p*-$CH_3C_6H_4CH(CH_3)_2$]; 22.2 [*p*-$CH_3C_6H_4CH(CH_3)_2$]; 30.7 [*p*-$CH_3C_6H_4CH(CH_3)_2$]; 49.2 and 49.7 (NCH_2CH_2N); 52.9 (-$NCH_2C_6H_5$); 56.0 (*s*, 2H, $NCH_2C_{10}H_7$); 80.6, 81.3, 96.8, 97.2, 101.2 and 107.4 (*p*-$CH_3C_6H_4CH(CH_3)_2$); 122.4, 123.0, 125.2, 126.3, 126.7, 127.7, 128.0, 128.7, 128.8, 131.1, 133.6, 133.8 and 137.1. (Ar–***C***); 209.8 (Ru–Cc_{arbene}).

2.1.2. Synthesis of dichloro[1-(2-methylbenzyl)−3-naphthyl-imidazolidin-2-ylidene](p-cymene) ruthenium(II), 1b

The complex **1b** was synthesized by performing the same procedure for the synthesis of complex **1a**. Here, the chloro[1-(2-methylbenzyl)−3-naphthyl-imidazolidin-2-ylidene]silver(I) (0.128 g, 0.28 mmol) was used as the starting material silver complex. Yield: 141 mg, (79%). m.p.: 214–215 °C; $\nu_{(CN)}$: 1447 cm^{-1}. Anal. Calc. for $C_{32}H_{36}Cl_2N_2Ru$: C:61.93; H:5.85; N:4.51. Found: C:62.37; H:6.04; N:4.46. ^1H NMR (300 MHz, $CDCl_3$); δ 1.01 and 1.14 (s, 6H, *p*-$CH_3C_6H_4CH(CH_3)_2$); 1.94 (*s*, 3H, *p*-$CH_3C_6H_4CH(CH_3)_2$); 2.32 (*s*, 3H, -$NCH_2C_6H_4(CH_3)$); 2.62 (*m*, 1H, *p*-$CH_3C_6H_4CH(CH_3)_2$); 3.46, 3.61 and 3.78 (s, 4H, NCH_2CH_2N); 5.27 and 5.40 (*d*, 4H, *J*: 5.9 and 5.9 Hz, *p*-$CH_3C_6H_4CH(CH_3)_2$); 5.04 (*s*, 2H, $NCH_2C_6H_4(CH_3)$); 5.18 (*s*, 2H, $NCH_2C_{10}H_7$); 7.04–8.06 (*m*, 11H, Ar–***H***); ^{13}C NMR (300 MHz, $CDCl_3$); δ 17.4 and 17.9 [*p*-$CH_3C_6H_4CH(CH_3)_2$]; 20.5 (-$NCH_2C_6H_4(CH_3)$); 21.1 [*p*-$CH_3C_6H_4CH(CH_3)_2$]; 29.6 [*p*-$CH_3C_6H_4CH(CH_3)_2$]; 48.1 and 48.6 (NCH_2CH_2N); 51.8 (-$NCH_2C_6H_4(CH_3)$); 54.9 (*s*, 2H, $NCH_2C_{10}H_7$); 79.5, 80.3, 95.9, 100.2 and 106.3 (*p*-$CH_3C_6H_4CH(CH_3)_2$); 121.4, 122.0, 123.8, 124.2, 125.3, 125.7, 126.9, 127.5, 127.6, 127.8, 130.1, 132.7,132.8, 136.4 and 137.4. (Ar–***C***); 208.8 (Ru–Cc_{arbene}).

2.1.3. Synthesis of dichloro[1-(4-methylbenzyl)−3-naphthyl-imidazolidin-2-ylidene](p-cymene) ruthenium(II), 1c

The complex **1c** was synthesized by performing the same procedure for the synthesis of complex **1a**. Here, the chloro[1-(4-methylbenzyl)−3-naphthyl-imidazolidin-2-ylidene]silver(I) (0.128 g, 0.28 mmol) was used as the starting material silver complex. Yield: 144 mg, (81%). m.p.: 207–208 °C; $\nu_{(CN)}$: 1448 cm^{-1}. Anal. Calc. for $C_{32}H_{36}Cl_2N_2Ru$: C:61.93; H:5.85; N:4.51. Found: C:62.19; H:6.07; N:4.46. ^1H NMR (300 MHz, $CDCl_3$); δ 1.09 and 1.22 (s, 6H, *p*-$CH_3C_6H_4CH(CH_3)_2$); 2.03 (*s*, 3H, *p*-$CH_3C_6H_4CH(CH_3)_2$); 2.37 (*s*, 3H, -$NCH_2C_6H_4(CH_3)$); 2.72 (*m*, 1H, *p*-$CH_3C_6H_4CH(CH_3)_2$); 3.53, 3.68 and 3.85 (*s*, 4H, NCH_2CH_2N); 5.11 (*s*, 2H, $NCH_2C_6H_4(CH_3)$); 5.27 (*s*, 2H, $NCH_2C_{10}H_7$); 5.35 and 5.49 (*d*, 4H, *J*: 5.9 and 5.9 Hz, *p*-$CH_3C_6H_4CH(CH_3)_2$); 7.19–8.15 (*m*, 11H, Ar–***H***); ^{13}C NMR (300 MHz, $CDCl_3$); δ 18.5 and 18.9 [*p*-$CH_3C_6H_4CH(CH_3)_2$]; 21.1 [*p*-$CH_3C_6H_4CH(CH_3)_2$]; 22.2 (-$NCH_2C_6H_4(CH_3)$); 30.6 [*p*-$CH_3C_6H_4CH(CH_3)_2$]; 49.1 and 49.6 (NCH_2CH_2N); 52.8 (-$NCH_2C_6H_4(CH_3)$); 55.7 (*s*, 2H, $NCH_2C_{10}H_7$); 80.5, 81.3, 96.8, 100.2 and 107.3 (*p*-$CH_3C_6H_4CH(CH_3)_2$); 122.4, 123.0, 125.2, 126.3, 126.7, 127.9, 128.8, 129.4,131.1, 133.7, 133.8, 134.0 and 137.3. (Ar–***C***); 209.6 (Ru–Cc_{arbene}).

2.1.4. Synthesis of dichloro[1-naphthyl-3-(2,3,5,6-tetramethylbenzyl)imidazolidin-2-ylidene](p-cymene)ruthenium(II), 1d

The complex **1d** was synthesized by performing the same procedure for the synthesis of complex **1a**. Here, the chloro[1-naphthyl-3-(2,3,5,6-tetramethylbenzyl)imidazolidin-2-ylidene]silver(I) (0.128 g, 0.28 mmol) was used as the starting material silver complex. Yield: 145 mg, (78%). m.p.: 265–266 °C; $\nu_{(CN)}$: 1448 cm^{-1}. Anal. Calc. for $C_{35}H_{42}Cl_2N_2Ru$: C:63.43; H:6.39; N:4.23. Found: C:63.69; H:6.52; N:4.17. ^1H NMR (300 MHz, $CDCl_3$); δ 1.15 and 1.27 (s, 6H, *p*-$CH_3C_6H_4CH(CH_3)_2$); 2.06 (*s*, 3H, *p*-$CH_3C_6H_4CH(CH_3)_2$); 2.28 and 2.38 (*s*, 12H, -$NCH_2C_6H(CH_3)_4$); 2.76 (*m*, 1H, *p*-$CH_3C_6H_4CH(CH_3)_2$); 3.30, 3.53 and 3.67 (*s*, 4H, NCH_2CH_2N); 5.24 (*s*, 2H, $NCH_2C_6H(CH_3)_4$); 5.41 and 5.49 (*s*, 4H, *p*-$CH_3C_6H_4CH(CH_3)_2$); 6.11 (*s*, 2H, $NCH_2C_{10}H_7$); 7.00 (*s*, 1H, -$NCH_2C_6H(CH_3)_4$); 7.28–8.13 (*m*, 7H, Ar–***H***); ^{13}C NMR (300 MHz, $CDCl_3$); δ 16.5 [*p*-$CH_3C_6H_4CH(CH_3)_2$]; 18.5 [*p*-$CH_3C_6H_4CH(CH_3)_2$]; 20.5 and 22.7 (-$NCH_2C_6H(CH_3)_4$); 30.9 [*p*-$CH_3C_6H_4CH(CH_3)_2$]; 48.7 and 48.9 (NCH_2CH_2N); 49.7 (-$NCH_2C_6H(CH_3)_4$); 53.0 (*s*, 2H, $NCH_2C_{10}H_7$); 85.3, 96.3, and 106.4 (*p*-$CH_3C_6H_4CH(CH_3)_2$); 122.2, 123.0, 125.2, 126.3, 126.6, 127.7, 128.8, 131.1, 131.7, 132.4, 133.8 and 133.9. (Ar–***C***); 209.3 (Ru–Cc_{arbene}).

2.2. The Anticancer Activity Determination of The Synthesized Complexes

HepG2 (liver cancer cell line) cells were cultured in a medium (DMEM) containing 10% fetal bovine serum (FBS) and 1% Penicillin/Streptomycin solution (10,000 units penicillin and 10 mg streptomycin/mL) with an incubator having 5% CO_2 at 37 °C. The cultured cells were seeded in 96-well plates with a density of 10^4 and incubated for 24 h under the same conditions. The complexes were dissolved in DMEM medium containing no more than one percent of DMSO and dilutions of the solutions at the specified concentrations as 6.25, 12.5, 25, 50, 100, 200 µM were carried out with DMEM medium. The medium of the cells attached onto 96-well plates was replaced with solutions of the complexes. The media in control wells were replaced with fresh medium. The prepared complex-cell system was incubated for 24 h under the same conditions. Then, the medium was removed and a mixture of 10 µL MTT (5 mg/mL) and 90 µL DMEM was added onto the adhered cells. After incubation under the same conditions for 4 h in dark, 100 µL DMSO was added after discarding the solution on cells and absorbance measurements were carried out in Biotek Eon microplate reader at 540 nm. The control wells were considered as 100% alive. Based on the absorbance results, IC_{30} (The cytostatic concentration), which is defined as 30% of reducing in cell reproduction activity via using an active substance which is mostly applied for cancer treatment, and IC_{50} (The half of maximal inhibitory concentration), which is a inhibiting potential measurement of a substance against a specific biological or biochemical material, values of the complexes were found.

2.3. Revealing DNA Interaction Models of The Synthesized Complexes

2.3.1. The determination of DNA interactions using agarose gel electrophoresis

The DNA binding activities of the ruthenium complexes were investigated using agarose gel electrophoresis technique via pBR322 plasmid DNA. Since **1a**, **1b**, **1c**, and **1d** complexes are insoluble in water, we used DMSO as the solvent. The test samples were diluted in different final concentrations as 25, 50, and 100 µg/mL with 4 µL addition of pBR322 plasmid DNA (the final concentration

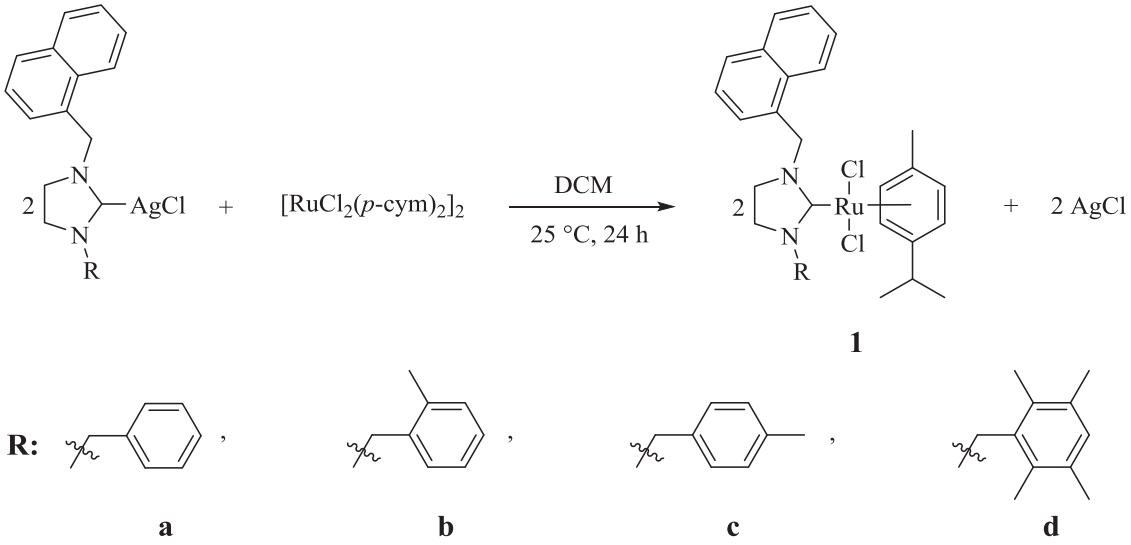

Scheme 1. Synthesis of imidazolidine-functionalized Ru(II)NHC complexes bearing naphthyl substitute **1a**-**d**.

in the solution is 0.025 µg/mL). Cisplatin was used as positive control. The different concentrated samples were incubated for 24 h at 37 °C. After incubation period, gel loading dye was added into each tube and the complexes were loaded into the wells of the previously prepared 1% of agarose gel. Electrophoresis procedure was occured at 75 V during 40 min. Then, the gel was stained with EtBr and the photo was taken using Syngene G:BOX gel documentation system.

The DNA binding properties of the synthesized complexes were investigated with pBR322 DNA. When DNA binding was happened, the supercoiled form (I) of pBR322 DNA structure was changed into the nicked form (II). The relatively rapid migration of intact supercoiled DNA form (I) is occured compared to the nicked DNA form (II), which binded to any complex, during electrophoresis.

2.3.2. The determination of DNA interactions with fluorescence spectrophotometer

In this ethidium bromide (EtBr) exchanging also known as EtBr fluorescence quenching assay, stock solutions of **1a**, **1b**, **1c**, and **1d** ruthenium complexes were prepared using dimethyl sulfoxide (DMSO). Then, using Tris–HCl buffer, all complexes were diluted as 12.5, 25, 50, 100, 150, 200, and 250 µg/mL from the master stock. The main stock of calf thymus DNA (calf thymus DNA-*ct*DNA) was prepared as 1 mg/mL in Tris–HCl buffer. The concentration ratio of *ct*DNA/EtBr was adjusted to 10 in each well of the 96-well plate, and *ct*DNA was pretreated with EtBr. Then, solutions prepared with different concentrations of ruthenium complexes were respectively added on top of the mixture of *ct*DNA and EtBr in each well of the 96-well plate. After incubating for half an hour at room temperature, the 96-well plate was measured in the range of 575–700 nm at 545 nm excitation wavelength using a multi-mode microplate reader named BioTek Synergy™ H1.

3. Results and Discussion

The imidazolidine-functionalized Ru(II)NHC complexes **1a-d** containing naphthyl substitute group were synthesized from Ag(I)NHC complexes containing naphthyl substitute $[RuCl_2(p\text{-cymene})]_2$ via transmetallation method (Scheme 1). The Ru(II)NHC complexes were obtained as a red-brown solid in 78% to 84% yield. All Ru(II)NHC complexes were air and moisture resistant. All Ru(II)NHC complexes were dissolved in halogenated (such as chloroform and dichloromethane) and polar solvents (such as dimethylformamide and dimethyl sulfoxide). They were less soluble in protic solvents such as water and alcohol. Also, they were partially dissolved in toluene which is apolar. The formations of the imidazolidine-functionalized Ru(II)NHC complexes **1a-d** were confirmed by ^{1}H NMR, ^{13}C NMR, and FT-IR spectroscopic methods and elemental analysis techniques. All spectra of the synthesized Ru(II)NHC complexes are consistent with the proposed formula. NMR spectra show that the Ru–$C_{carbene}$ resonances of the Ru(II)NHC complexes in the ^{13}C NMR spectra appeared highly downfield shifted at δ 209.8, 208.8, 209.6 and 209.3 ppm for **1a-d**, respectively. Also, the results of the elemental analysis calculated with the experimental elemental analysis results of Ru(II)NHC complexes **1a-d** were observed very closer to each other. The FT-IR data clearly indicated the presence of ν(CN) at 1450, 1447, 1448, and 1448 cm^{-1} for these complexes **1a-d**, respectively. The spectroscopic data obtained for the imidazolidine-functionalized Ru(II)NHC complexes **1a-d** containing naphthyl substitute group are compatible with the literature [8,34,38].

Table 1
IC_{30} and IC_{50} values of the synthesized complexes against HepG2 cell line.

Complex	IC_{30}, µM (HepG2)	IC_{50}, µM (HepG2)
1a	41.82 ± 2.53	84.27 ± 2.00
1b	41.60 ± 1.42	103.81 ± 0.28
1c	78.36 ± 11.47	133.56 ± 0.73
1d	23.90 ± 0.32	32.84 ± 0.44
Cisplatin	91.64 ± 12.18	147.97 ± 7.70

From the data on Table 1, all the synthesized compounds showed high anticancer activities with presenting lower IC_{30} and IC_{50} values compared to cisplatin against liver cancer cell line, HepG2. In particular, the compound **1d** presented the highest anticancer activity, while **1a** and **1b** had similar IC_{30} values. The reason for the difference in IC_{50} values of these complexes is thought to be since **1a** exhibits a steeper linear curve than **1b** and therefore, this complex **1a** kills more cells compared to **1b** at high concentrations. Compared to other complexes, **1c** has the highest cytostatic and cytotoxic values. All of these values are smaller than cisplatin. In order to kill cancer cells which means exhibiting anticancer activities, our Ru(II)NHC complexes has to pass through the cell membrane because of their hydrophobic characteristics.

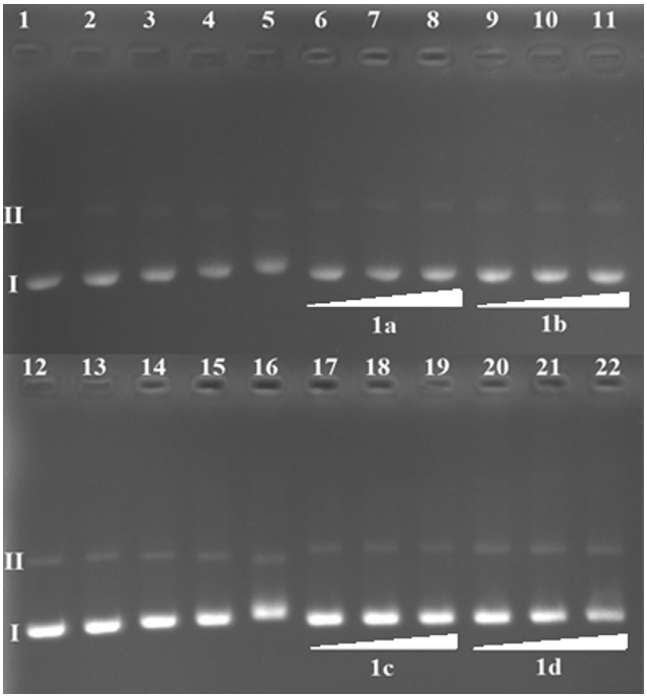

Fig. 1. The agarose gel electrophoresis image shows changes in the supercoiled DNA form (I) and the open circular DNA form (II) of plasmid pBR322 (lanes 1, 2, 12, and 13) after 24 h incubation at 37 °C with the final concentrations of 25, 50, and 100 μg/mL cisplatin controls (lanes 3, 4, 5 and 14, 15, 16), 25, 50, and 100 μg/mL concentrations of **1a** complex (lanes 6, 7, and 8), **1b** complex (lanes 9, 10, and 11), **1c** complex (lanes 17, 18, and 19), and **1d** complex (lanes 20, 21, and 22), respectively.

The steric bulky of the Ru(II)NHC complexes (**1a-d**) as well as their electronic interactions with the cancer cells and DNA chain are important in the biological activities of complexes. Ru(II)NHC complexes **1a-d** must be able to pass through the cell membrane with their lipophilic (hydrophobic) characteristics in order to affect cancer cells. These complexes exhibit higher activities if they pass through membrane into the cell. When the biological activity results are analyzed, it is seen that in anticancer activity against HepG2 cell line, **1c** shows the lowest activity. When Ru(II)NHC complexes **1a-d** are examined, it is seen that tetramethyl substituted complex **1d** having the most hydrophobic structure shows the highest anticancer activity against HepG2 cells. The two Ru(II)NHC complexes **1b** and **1c** are structural isomers and exhibit anticancer activities against HepG2 cell line. According to this result, the lipophilic properties of these complexes are decisive in anticancer activities.

The complexes can either get close to DNA helix, interact with DNA grooves, and then bond with DNA with secondary bonds (Van der Waals interactions) [37] or chemically bond to DNA molecules with alkyl groups on them [36]. For these interactions to be sufficient, Ru(II)NHC complexes must approach or enter DNA grooves. As steric volumes of the complexes shrink, they will get closer to approach or interact with DNA minor/major grooves.

The slightly binding properties of **1a**, **1b**, **1c**, and **1d** ruthenium complexes to pBR322 plasmid DNA were observed. Increased concentrations of **1a** and **1b** supercoiled form (I) of the plasmid run rapidly compared to the others unlike **1c** and **1d** In addition, the band patterns for **1a** are similar to **1b** in contrast to **1c** and **1d** ruthenium complexes. As seen in Fig. 1, cisplatin controls have effects on all the forms of pBR322 plasmids (lanes 3, 4, 5, 14, 15, and 16) compared to the pure pBR322 plasmids (lanes 1, 2, 12, and 13).

Table 2
*ct*DNA quenching coefficients (K_{SV}) of the complexes **1a**-**1b**-**1c**-**1d** in EtBr exchanging assay.

Complex	K_{SV} [M^{-1}] x 10^{-2}
1a	4.13 ± 0.50
1b	9.11 ± 0.12
1c	2.79 ± 0.43
1d	3.92 ± 0.23

The *ct*DNA quenching coefficients (K_{SV}) of the synthesized complexes were determined by EtBr exchanging assay (Table 2). By adding **1a**, **1b**, **1c**, and **1d** complexes in increasing concentrations onto EtBr bound to *ct*DNA, it is clearly seen from Fig. 2 that EtBr's emission intensity decreases in the order of complexes. This shows that the binding of complexes to DNA is intercalated, that is, between the bases, or to the minor grooves of DNA [41–45]. The ability of complexes to quench, namely binding to DNA, is evaluated with the Stern-Volmer quenching constant (K_{SV}) [46,47].

$F_0/F = 1 + K_{SV}\,[Q] = 1 + \kappa_q\,\tau_0\,[Q]$

F_0: Fluorescence intensity without complex κ_q: The quenching rate coefficient

F: Fluorescence intensity with complex [Q]: Concentration of the complex

τ_0: Average lifetime of the EtBr-*ct*DNA-linked complex in the absence of quencher ($\tau_0 = 10^{-8}$ s)

DNA interactions of Ru(II)NHC complexes can be explained by different mechanisms. Some metal complexes, such as ruthenium (II), electrostatically bind to DNA from the negatively charged sugar-phosphate backbone of the nucleic acid. Furthermore, mostly multi-ring, aromatic, and planar structures are used to dye nucleic acids [37]. Therefore, it is obvious that multi-ring, planar, and aromatic structures such as benzene and naphthyl in the structure of Ru(II)NHC complexes will increase the interaction with DNA. As a result, when complexes are examined in terms of DNA binding according to the K_{SV} values obtained from Table 2, it is seen that **1b** has the highest DNA binding property compared to other complexes. However, **1a**, **1c**, and **1d** have very similar properties in terms of DNA binding via the EtBr-*ct*DNA system. Since it has less steric bulky, it can be assumed that **1a-c** complexes can be closer to the DNA helix than **1d** complex. Furthermore, it can be related to the interaction difference of **1b** (*ortho*-methyl) and **1c** (*para*-methyl) complexes on the DNA helix to the position isomerism (*ortho*/*para*) in each complex [48]. The interactions between complex **1b** and DNA helix are considered to be high due to this position isomerism.

4. Conclusions

We have reported the synthesis of the imidazolidine-functionalized Ru(II)NHC complexes **1a-d** containing naphthyl substituent group and their structures were confirmed by using ^{1}H NMR, ^{13}C NMR, FTIR spectroscopic method and elemental analysis techniques. The biological activities of the novel complexes were investigated *in vitro*. By finding IC_{30} and IC_{50} values, anticancer activities of the synthesized complexes against HepG2 cell line were determined. The values of inhibited cell proliferation by fifty percent (IC_{50}) in terms of **1a** and **1d** have presented better anticancer activity results compared to other human cancer cell lines [49,50]. Moreover, DNA binding properties via observing band patterns on agarose gel and using a fluorescence spectrophotometer with EtBr exchanging assay were performed in order to understand the biological activities. Consequently, the complexes **1a** and **1b** had similar anticancer (in terms of IC_{30}) and DNA

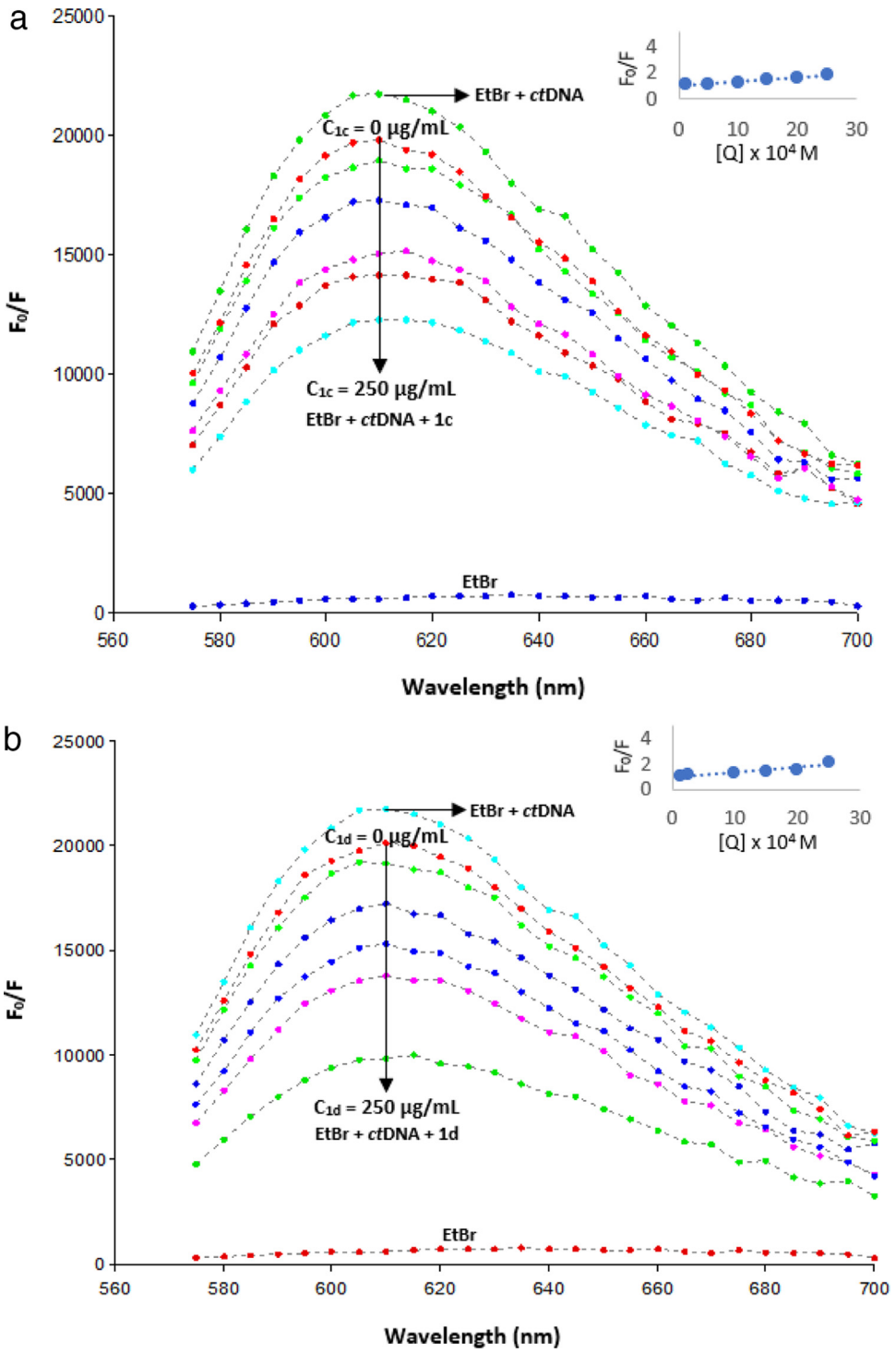

Fig. 2. Fluorescence emission spectra of different concentrations for the complexes **1a**-**1b**-**1c**-**1d** in the EtBr-*ct*DNA system.

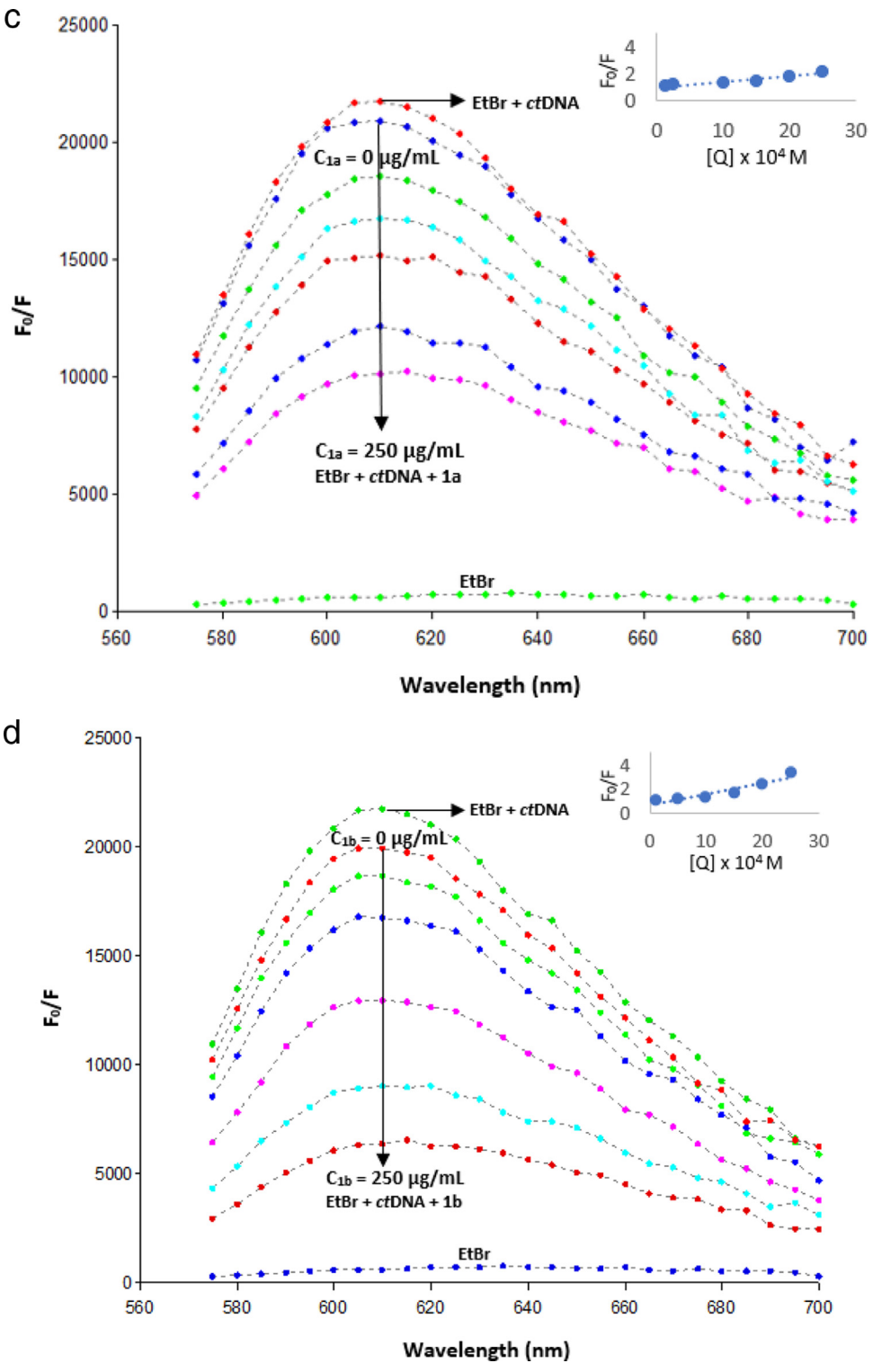

Fig. 2. Continued

binding activities. In addition, **1b** had the highest DNA binding property as an intercalative manner. Unlike **1b**, **1d** may attach to cell membrane and disrupt its integrity.

Declaration of Competing Interest

The authors have declared no conflict of interest.

CRediT authorship contribution statement

Canbolat Gürses: Methodology, Writing – original draft, Software. **Aydın Aktaş:** Methodology, Data curation, Writing – original draft. **Sevgi Balcıoğlu:** Methodology, Writing – original draft. **Araniy Fadhilah:** Methodology. **Yetkin Gök:** Conceptualization, Writing – review & editing. **Burhan Ateş:** Investigation, Conceptualization.

Acknowledgement

This work was financially supported by İnönü University Research Fund (IUBAP FBG-2018–1569). The authors acknowledge İnönü University Scientific and Technology Center for the elemental analyses of the compounds and the authors acknowledge İnönü University Faculty of Science Department of Chemistry for the characterization of compounds.

Supplementary materials

Supplementary material associated with this article can be found, in the online version, at doi:10.1016/j.molstruc.2021.131350.

References

[1] C. Chen, S. Ni, Q. Zheng, M. Yu, H. Wang, Synthesis, structure, biological evaluation, and catalysis of two pyrazole-functionalized NHC–Ru^{II} complexes, Eur. J. Inorg. Chem. (2017) 616–622.
[2] B. Rosenberg, L. VanCamp, J.E. Trosko, V.H. Mansour, Platinum compounds: a new class of potent antitumour agents, Nature 222 (1969) 385–386.
[3] M.G. Karaaslan, A. Aktaş, C. Gurses, B. Ateş, Y. Gök, Chemistry, structure, and biological roles of Au-NHC complexes as TrxR inhibitors, Bioorg. Chem. 95 (2020) 103552.
[4] A. Aktaş, Ü. Keleştemur, Y. Gök, S. Balcıoğlu, B. Ateş, M. Aygün, 2-Morpholinoethyl-substituted *N*-heterocyclic carbene (NHC) precursors and their silver(I)NHC complexes: synthesis, crystal structure and in vitro anticancer properties, J. Iran Chem. Soc. 15 (1) (2018) 131–139.
[5] S.A. Patil, A.P. Hoagland, S.A. Patil, A. Bugarin, *N*-heterocyclic carbene-metal complexes as bio-organometallic antimicrobial and anticancer drugs, an update (2015–2020), Future Med Chem 12 (2020) 24.
[6] T. Scattolin, E. Bortolamiol, F. Rizzolio, N. Demitri, F. Visentin, Allyl palladium complexes bearing carbohydrate-based N-heterocyclic carbenes: Anticancer agents for selective and potent in vitro cytotoxicity, Appl Organomet Chem 34 (10) (2020) e5876.
[7] N. Touj, İ.S. Al Nasr, W.S. Koko, T.A. Khan, İ. Özdemir, S. Yasar, L. Mansour, F. Alresheedi, N. Hamdi, Anticancer, antimicrobial and antiparasitical activities of copper(I) complexes based on *N*-heterocyclic carbene (NHC) ligands bearing aryl substituents, J Coord Chem 73 (20–22) (2020) 2889–2905.
[8] Y. Sarı, C. Gürses, D.B. Celepci, Ü. Keleştemur, A. Aktaş, Ş. Yüksel, B. Ateş, Y. Gök, 4-Vinylbenzyl and 2-morpholinoethyl substituted ruthenium (II) complexes: Design, synthesis, and biological evaluation, J Mol Struct 1202 (2020) 127355.
[9] N.P. Barry, P.J. Sadler, Challenges for metals in medicine: how nanotechnology may help to shape the future, ACS Nano 7 (2013) 5654–5659.
[10] S. Thota, S. Vallala, R. Yerra, E.J. Barreiro, Design, synthesis, characterization, cytotoxic and structure activity relationships of novel Ru (II) complexes, Chinese Chem. Lett. 26 (2015) 721–726.
[11] B. Feng, E. Sundin, P. Lincolna, A.K.F. Mårtensson, DNA threading intercalation of enantiopure [Ru (phen) 2 bidppz] 2^+ induced by hydrophobic catalysis, Phys. Chem. Chem. Phys. 23 (2021) 2238–2244.
[12] A. Mondal, U. Sen, N. Roy, V. Muthukumar, S.K. Sahoo, B. Bose, P. Paira, DNA targeting half sandwich Ru (II)-p-cymene-N^ N complexes as cancer cell imaging and terminating agents: influence of regioisomers in cytotoxicity, Dalton Trans 50 (2021) 979–997.
[13] F.E. Poynton, S.A. Bright, S. Blasco, D.C. Williams, J.M. Kelly, T. Gunnlaugsson, The development of ruthenium(II) polypyridyl complexes and conjugates for *in vitro* cellular and *in vivo* applications, Chem. Soc. Rev. 46 (2017) 7706–7756.
[14] A. Notaro, G. Gasser, Monomeric and dimeric coordinatively saturated and substitutionally inert Ru (II) polypyridyl complexes as anticancer drug candidates, Chem. Soc. Rev. 46 (2017) 7317–7337.
[15] S. Thota, D.A. Rodrigues, D.C. Crans, E.J. Barreiro, Ru (II) compounds: next-generation anticancer metallotherapeutics? J. Med. Chem. 61 (2018) 5805–5821.
[16] C.S. Allardyce, P.J. Dyson, Ruthenium in medicine: current clinical uses and future prospects, Platinum Met. Rev. 45 (2001) 62–69.
[17] E. Alessio, Thirty years of the drug candidate NAMI-A and the myths in the field of ruthenium anticancer compounds: a personal perspective, Eur. J. Inorg. Chem. 12 (2017) (2017) 1549–1560.
[18] M.J. Clarke, F. Zhu, D.R. Frasca, Non-platinum chemotherapeutic metallopharmaceuticals, Chem. Rev. 99 (1999) 2511–2534.
[19] M. Clarke, Ruthenium metallopharmaceuticals, Coord. Chem. Rev. 236 (2003) 209–233.
[20] C.G. Hartinger, S. Zorbas-Seifried, M.A. Jakupec, B. Kynast, H. Zorbas, B.K. Keppler, From bench to bedside – preclinical and early clinical development of the anticancer agent indazolium trans-[tetrachlorobis(1H-indazole)ruthenate(III)] (KP1019 or FFC14A), J. Inorg. Biochem. 100 (2006) 891–904.
[21] S.M. Meier-Menches, C. Gerner, W. Berger, C.G. Hartinger, B.K. Keppler, Structure–activity relationships for ruthenium and osmium anticancer agents–towards clinical development, Chem. Soc. Rev. 47 (2018) 909–928.
[22] A. Weiss, R.H. Berndsen, M. Dubois, C. Müller, R. Schibli, A.W. Griffioen, P.J. Dyson, P. Nowak-Sliwinska, *In vivo* anti-tumor activity of the organometallic ruthenium(II)-arene complex [Ru(η^6-*p*-cymene)- Cl_2(pta)] (RAPTA-C) in human ovarian and colorectal carcinomas, Chem. Sci. 5 (2014) 4742–4748.
[23] W. Liu, R. Gust, Metal *N*-heterocyclic carbene complexes as potential antitumor metallodrugs, Chem. Soc. Rev. 42 (2013) 755–773.
[24] K. Suntharalingam, S.G. Awuah, P.M. Bruno, T.C. Johnstone, F. Wang, W. Lin, Y. Zheng, J.E. Page, M.T. Hemann, S.J. Lippard, Necroptosis-Inducing Rhenium(V) Oxo Complexes, J. Am. Chem. Soc. 137 (2015) 2967–2974.
[25] A.A. Nazarov, C.G. Hartinger, P.J. Dyson, Opening the lid on piano-stool complexes: An account of ruthenium(II)–arene complexes with medicinal applications, J. Organomet. Chem. 751 (2014) 251–260.
[26] N.Y.S. Lam, D. Truong, H. Burmeister, M.V. Babak, H.U. Holtkamp, S. Movassaghi, D.M. Ayine-Tora, A. Zafar, M. Kubanik, L. Oehninger, T. Söhnel, J. Reynisson, S.M.F. Jamieson, C. Gaiddon, I. Ott, C.G. Hartinger, From Catalysis to Cancer: Toward Structure–Activity Relationships for Benzimidazol-2-ylidene-Derived *N*-Heterocyclic-Carbene Complexes as Anticancer Agents, Inorg. Chem. 57 (2018) 14427–14434.
[27] F. Türker, C. Gürses, D.B. Celepci, A. Aktaş, B. Ateş, Y. Gök, New morpholine-liganded palladium(II) *N*-heterocyclic carbene complexes: Synthesis, characterization, crystal structure, and DNA-binding studies, Archiv der Pharmazie (2019) 1900187.
[28] F. Erdemir, D.B. Celepci, A. Aktaş, Y. Gök, Synthesis, crystal structures, spectral investigations, conformational analysis and DFT studies of *N*- heterocyclic carbene precursors, J Mol Struct 1204 (2020) 127519.
[29] A. Aktaş, D.B. Celepci, Y. Gök, Synthesis, crystal structures, spectral FT-IR, NMR and UV–Vis investigations and Hirshfeld surface analysis of two new 2-hydroxyethyl-substituted *N*-heterocyclic carbene precursors, J. Chinese Chem. Soc. 66 (10) (2019) 1389–1396.
[30] A. Aktaş, P. Taslimi, Y. Gök, İ. Gülçin, Novel NHC Precursors: Synthesis, Characterization, and Carbonic Anhydrase and Acetylcholinesterase Inhibitory Properties, Archiv der Pharmazie 6 (2017) 350.
[31] A. Aktaş, S.A.A. Noma, D.B. Celepci, F. Erdemir, Y. Gök, B. Ateş, New 2-hydroxyethyl substituted N-Heterocyclic carbene precursors: Synthesis, characterization, crystal structure and inhibitory properties against carbonic anhydrase and xanthine oxidase, J Mol Struct 1184 (2019) 487–494.
[32] S. Bal, A. Aktaş, R. Kaya, Y. Gök, M. Karaman, P. Taslimi, İ. Gülçin, Novel 2-methylimidazolium salts: Synthesis, characterization, molecular docking, and carbonic anhydrase and acetylcholinesterase inhibitory properties, Bioorg. Chem. (2020) 103468.
[33] P.K. Anuja, P. Paira, Luminescent anticancer Ru(II)-arenebipyridine and phenanthroline complexes: Synthesis, characterization, DFT studies, biological interactions and cellular imaging application, J. Inorg. Biochem. 208 (2020) 111099.
[34] O. Tokgun, D.E. Karakas, S. Tan, E.R. Karagür, B. Inal, H. Akca, F. Durap, A. Baysal, M. Aydemir, Novel ruthenium and palladium complexes as potential anticancer molecules on SCLC and NSCLC cell lines, Chemical Papers 74 (2020) 2883–2892.
[35] E.J. Sammriski, D.C. Schwartz, J.J. de Pablo, A mesoscale model of DNA and its renaturation, Biophys. J. 96 (2009) 1675–1690.
[36] S. Thota, S. Vallala, R. Yerra, D.A. Rodrigues, N.M. Raghavendra, E.J. Barreiro, Synthesis, characterization, DNA binding, DNA cleavage, protein binding and cytotoxic activities of Ru(II) complexes, Int. J. Biol. Macromol. 82 (2016) 663–670.
[37] S.S. Karki, S. Thota, S.Y. Darj, J. Balzarini, E.D. Clercq, Synthesis, anticancer, and cytotoxic activities of some mononuclear Ru(II) compounds, Bioorg. Med. Chem. 5 (2007) 6632–6641.
[38] A. Mukherjee, T. Chaudhuri, S. Moulik, M. Banerjee, Internal charge transfer based ratiometric interaction of anionic surfactant with calf thymus DNA bound cationic surfactant: Study I, Spectrochimica Acta Part A 152 (2016) 1–7.
[39] M. Top, O. Er, G. Congur, A. Erdem, F. Lammrecht, Intracellular uptake study of radiolabeled anticancer drug and impedimetric detection of its interaction with DNA, Talanta 160 (2016) 157–163.
[40] M. Lee, L. Rhodes, M.D. Wyatt, S. Forrow, J.A. Hartley, GC base sequence recognition by oligoimidazolecarboxamide and C-terminus-modified analogs of distamycin deduced from circular dichroism, proton nuclear magnetic resonance, and methidiumpropylethylenediaminetetraacetate-iron(II) footprinting studies, Biochemistry 32 (1993) 4237–4245.
[41] D.A. Barawkar, K.N. Ganesh, Fluorescent d(CGCGAATTCGCG): characterization of major groove polarity and study of minor groove interactions through a major groove semantophore conjugate, Nucleic Acids Res 23 (1995) 159–164.
[42] R. Palchaudhuri, P.J. Hergenrother, DNA as a target for anticancer compounds: methods to determine the mode of binding and the mechanism of action, Current Opin. Biotechnol 18 (2007) 497–503.
[43] T. Afrati, A.A. Pantazaki, C. Dendrinou-Samara, C. Raptopoulou, A. Terzis, D.P. Kessissoglou, Copper inverse-9-metallacrown-3 compounds interacting with DNA, Dalton Trans 39 (2010) 765–775.
[44] S. Anbu, M. Kandaswamy, S. Kamalraj, J. Muthumarry, B. Varghese, Phosphatase-like activity, DNA binding, DNAhydrolysis, anticancer and lactate dehydrogenase inhibition activity promoting by a new bis–phenanthroline dicopper(II) complex, Dalton Trans 40 (2011) 7310–7318.
[45] O. Stern, M.Z. Volmer, über die Abklingzeit der Fluoreszenz, Phys 20 (1919) 183–188.
[46] R. Kozlowski, R.F. Pettifer, J.M. Thomas, X-ray absorption fine structure investigation of vanadium(V) oxide-titanium(IV) oxide catalysts. 2. The vanadium oxide active phase, Phys. Chem. 87 (1983) 5176–5181.

[47] J.R. Lakowitcz, Dynamics of Solvent and Spectral Relaxation, in: Principles of Fluorescence Spectroscopy, Plenum Press, New York, 1999, pp. 237–259.
[48] J. Kladnik, S. Ristovski, J. Kljun, A. Defant, I. Mancini, K. Sep˘cić, I. Turel, Structural Isomerism and Enhanced Lipophilicity of Pyrithione Ligands of Organoruthenium(II) Complexes Increase Inhibition on AChE and BuChE, Int. J. Mol. Sci. 21 (2020) 5628.
[49] G. Lv, L. Guo, L. Qui, H. Yang, T. Wang, Liu H, J. Lin, Lipophilicity-dependent ruthenium N-heterocyclic carbene complexes as potential anticancer agents, Dalton Trans. 44 (2015) 7324–7331.
[50] C. Chen, C. Xu, T. Li, S. Lu, F. Luo, H. Wang, Novel NHC-coordinated ruthenium(II) arene complexes achieve synergistic efficacy as safe and effective anticancer therapeutics., Eur J Med Chem 203 (2020) 112605.